

---

---

# Dynamic Structural Health Monitoring With Filter Net De-noising and SSDBN Model Using Vibrational Data

**Pradeep Kumar. S**

*Department of Civil, Noorul Islam Center for Higher Education, Kumaracoil, KK Dist. TN, India.*  
E-mail: Predheep2003@yahoo.com

**M. Beena Mol**

*Department of Civil, LBS College of Engineering, Kasargod, Kerala, India.*

(Received 18 May 2023; accepted 25 July 2023)

Measurement noise is always part of the vibration data in vibration-based structural health monitoring (SHM). However, it might be challenging to regulate the state in which civil constructions are tested in the field. Moreover, strong noise from a variety of sources, make damage detection inaccurate. Additionally, the precision of the current studies will eventually begin to saturate and possibly deteriorate. To overcome the mentioned limitations, this research proposed a deep learning framework for monitoring the structural health. First, Filter Net is suggested, which integrates neural network techniques for de-noising observed vibration signals with skip connection, dropout and shuffling. The next step was to propose a smooth sparse deep boltzmann network to detect structural degradation. A sparse penalty component built on the inverse function norm was added to improve performance. In addition, a greedy algorithm is used to perform unsupervised learning, which trains the first Restricted Boltzmann Machines (RBM) using the sampling data before using the first RBM's parameters to initialize the Deep belief networks (DBNs) first layer's parameters. Then, a BP network is used in a fine-tuning method to get the final systematic parameters. As a result, the RBM provides the Smooth Sparse Deep Boltzmann Network (SSDBN) with a decent starting value and therefore ensures higher performance.

---

## NOMENCLATURE

$E$	energy function
$vis_i$	the binary state of the visible unit $i$
$c_i$	the bias weight of $vis_i$
$hid_j$	the binary state of the hidden unit $j$
$b_j$	the bias weight of $hid_j$
$w_{ij}$	the collection weight of the hidden layer $hid_j$ and the visionary layer $vis_i$
$m, n$	total number of the visible and hidden units
$\lambda$	model parameter of the RBM
$z$	partition function
$\eta$	step size
$\langle \rangle_{data}$	probability distribution of $prob(vis, hid; \lambda)$
$\langle \rangle_{recon}$	probability in relation to the model distribution
$x_o$	observed data
$prob(hid_{L-1} \vee hid_L)$	conditional probability of $hid_{L-1}$
$\hat{y}$	dependent variable's anticipated or forecast value
$U_o$	value of $\hat{y}$ when every independent variable

$X_1$ through $X_m$	separate predictor or independent variables
$U_1$ through $U_m$	regression coefficients
$\varepsilon$	random error

## 1. INTRODUCTION

The recent civil engineering structure disasters that resulted in tragic deaths and significant property damage have brought attention to the need for preventative measures to lessen the effects of structural failures. Damage to civil structures can decrease their stiffness and stability, which lowers the performance over their lifetime.<sup>1</sup> Utilizing a number of structural damage detection methods, an automated structural health monitoring (SHM) system that might provide advance notice of such structural deterioration has been developed.<sup>2</sup> Therefore, the evaluation of potential damage to structures in different permanent and/or accidental load scenarios is an important issue to be considered in rehabilitation decisions and emergency measure planning.<sup>3</sup> Potential damages can be found by employing processes for assessing the structural health, structural monitoring, and the use of methods for determining the dynamic characteristics of structures in the time or frequency domain. Any modification of a structure's dynamic characteristics noted by a monitoring procedure can be a sign that its

capacity to support loads has shrunk.<sup>4</sup>

The choice of extracted features and classifiers is crucial for the effectiveness of machine learning-based structural damage detection systems. A suitable classifier is essential for accurately classifying retrieved features based on their nature. Trial and error efforts have been made to identify the ideal combination of recovered characteristics and classifiers. The effectiveness of damage detection is affected by poor hand-crafted features and inadequate classifiers. Additionally, feature extraction and classification methods often require human labor and processing time, preventing the application of machine learning techniques in vibration-based structural damage detection for real-time SHM operations.

Deep belief networks (DBNs) are generative models trained utilising a sequence of stacked Restricted Boltzmann Machines (RBMs), or occasionally Auto encoders, along with one or more extra layers to create a Bayesian Network. There are no intra-layer connections due to the usage of RBMs (thus the "restricted" in Restricted Boltzmann Machines).<sup>9</sup> Additionally, the layers employ unsupervised pre-training utilising an RBM stacking process combining contrastive divergence because the initialization of the nodes has a significant impact on how well DBNs function. DBNs are frequently utilised for various categorization purposes as well.<sup>10</sup> The processing of vibration signals for various types of data in the time, frequency, and time-frequency domains has been the subject of recent research. For periodic signals, traditional time domain averaging techniques are better suited. since the variable vibration frequency or amplitude of signals, denoising's impact on other types of signals may be limited.<sup>11</sup> The removal of noise beyond the user-defined frequency range of attention involves using typical frequency domain filtering methods. Examples include low-pass filtering and band-pass filtering. The implementation of these approaches is restricted by the need for prior understanding of formations with modal frequencies and the fluctuation ranges that go along with them as a result of changes in operational and environmental variables.<sup>12</sup> The main contribution of this proposed deep learning framework for monitoring the structural health is as follows:

- This framework introduced FilterNet, to remove strong noise from a variety of sources, including ambient noise, measurement noise, and instrumental noise. The proposed FilterNet is integrated with skip connection, dropout, and shuffling approaches for denoising observed vibration signals by employing neural network.
- Following that, to identify structural damage, the Smooth Sparse Deep Boltzmann The suggested network incorporates a sparse penalty term based on the inverse function norm to enhance performance, and it also use BP network as a method for fine-tuning to obtain the final systematic parameters.

As a result, the suggested framework provides a higher performance when compared to the random initialization of the existing neural network.

The following describes the structure of this research study: Monitoring of the operational and structural health and dynamic assessments of building structures are covered in Section 2. The innovative method for determining structural damage using vibrational data was explained in Section 3. Moreover, Finally, Section 5 brings this research article to a close by discussing the outcomes of the recommended strategy that were mentioned in Section 4.

## 2. LITERATURE SURVEY

Hubbard et al.<sup>13</sup> compared and contrasted two distributed fibre optic sensing systems, based on Rayleigh in this research focused on how well they track the dynamic structural behaviour of a model wind turbine tower subject to both free and forced vibration. To examine if they can detect structural issues like loose bolts and material degradation inside the tower, they are also put through extra testing. Phase-based optical time domain reflectometry ( $\Phi$ -OTDR), a technique utilised in distributed acoustic sensing, and optical frequency domain reflectometry (OFDR) are the two techniques under investigation (DAS). Although OFDR is a tried-and-true strain measuring method, it can only detect strain over very small distances, which limits its applicability for structural health monitoring (10 s of meters). Utilizing the OFDR, the readings obtained with the  $\Phi$ -OTDR, which has a significantly larger measuring range, were confirmed (several kilometres). Because of its sensing distance capability,  $\Phi$ -OTDR is a viable approach for observing several wind turbines networked together with a single fibre optic cable.

Sivasuriyan et al.<sup>14</sup> looked at damage assessments for building structures as well as operational and structural health monitoring (SHM). The study addressed scenarios of evaluation and self-monitoring, involving damage detection, and assessed structures by installing sensors and assuming weak spots. From this aspect, a building may be continuously monitored in real time using cutting-edge sensor technology and data collecting methods. In order to forecast the damage, the response and behaviour of the structure were also monitored and noted. However, the models' data gathering and accuracy must be enhanced in future.

Maes et al.<sup>15</sup> looked at the viability of using natural frequencies to assess the structural health of a steel bowstring railroad bridge in Belgium. In particular, environmental influences that change the modal features of the structure, such as temperature, are removed. Two black-box modelling strategies that are used to eliminate natural frequency fluctuations brought on by changes in the environment are compared to one another. A receiver operating characteristic (ROC) curve analysis, which considers the actual refit as well as several other small structural adjustments that are depicted by a thorough finite element model of the structure, is used to evaluate the effectiveness of these procedures. Both the real refit and lesser structural alterations that cause only slight natural frequency changes show the state transition.

Liu et al.<sup>16</sup> focused on how a high-speed railway's ballasted

track construction continually carries the weight of moving vehicles, and the ballasted bed gradually dilutes and dissipates the vibration energy. A ballast sensor was created by integrating sensors within the ballast. It was placed on the ballasted rail in order to investigate structural health monitoring (SHM) during an impact excitation and to verify the co-simulation model using the Discrete Element Method (DEM) and Multi Body Dynamics (MBD). The findings shown that dispersed ballast sensors are capable of realising the SHM state of the ballasted track. The major vibration frequency of the ballast peaked at 153 Hz at the sleeper box, sleeper end, and ballast shoulder in response to an impact stimulation. Despite the reduction of the vibration amplitudes at the sleeper end and ballast shoulder, a secondary peak in the vibration amplitude of the ballast emerged at the sleeper box at double the frequency. The ballasted bed construction performed better at dampening vibrations in the low-frequency region than it did in the high-frequency regime. When high-frequency vibrations caused the surface layer of the ballast at the sleeper box to splash, the ballasted track structure's structural integrity was compromised. The ballasted bed's two sides take on the appearance of a "cyclone" under the rolling wheel load.

Jahan et al.<sup>17</sup> used an innovative hybrid Fuzzy Krill Herd technique to evaluate the general structural integrity of an operational bridge. Despite prior research on the algorithms, it is still unknown how well they might monitor the structural health of an actual bridge structure. Two different types of concrete and steel girder bridges are constructed in this article using the method. Finite element (FE) modelling was used to provide an extra numerical study on the dynamic characteristics and structural behaviour of the bridges. To determine if the suggested line of action is effective, basic two-dimensional girder simulation models and a three-dimensional FE model were utilised. The findings show that even with noisy input data or data that lacks values, the fuzzy logic technique may still gather reliable information. According to the findings, utilising torsional modes and increasing the number of measuring modes may accurately diagnose damage in symmetric structures.

Bedon et al.<sup>18</sup> presented unique homemade MEMS sensor prototypes in this work and validated them by first laboratory tests (shaking table experiments and noise level measurements). Following a discussion of their use for the dynamic identification of existing, full-scale structural assemblies based on the highly promising preliminary results, comparison calculations with earlier literature results are used to demonstrate their potential. These calculations include both on-site Experimental Modal Analysis (EMA) and Finite Element Analytical estimations (FEA). The case study for the full-scale experimental validation of MEMS accelerometers is the cable-stayed bridge at Pietratagliata (Italy). The study's dynamic findings, which are summarised below, show the MEMS accelerometers' extraordinary skill and suggest its applicability and promise in SHM applications. They also show evidence of relatively consistent and dependable predictions.

### 3. NOVEL DEEP LEARNING FRAMEWORK FOR MONITORING THE STRUCTURAL HEALTH

For an efficient and reliable condition assessment of structures, high-quality data with substantial dynamic vibration information of the structures and low-level noises in capacities are frequently needed. However, it might be challenging to regulate the state in which civil constructions are tested in the field. Strong noise from a variety of sources, including ambient noise, measurement noise, and instrumental noise, can readily corrupt measured dynamic responses. One major problem with deep learning-based approaches is that accuracy may eventually start to saturate and even worsen if the depth of networks keeps growing. Additionally, the precise distribution of damage must be known beforehand to calculate the joint probability. This is difficult since it requires a lot of answer information, yet only a tiny fraction of that data is related to several permutations of shaky connections that render the programme useless. To overcome the mentioned limitations this study focuses on developing a deep learning framework for monitoring the structural health by improving corrupted data, exploiting useful data, and forecasting various structural defects. To filter noise, this study produced FilterNet which is integrated with skip connection, dropout, and shuffling approaches for denoising observed vibration signals by employing neural network. In addition, to identify structural damage, the Smooth Sparse Deep Boltzmann Network was proposed. Here, a sparse penalty term based on the inverse function norm was added to improve performance, a greedy algorithm was used to perform unsupervised learning, BP network was then used in a fine-tuning method to get the final systematic parameters, and to further anticipate the structure's health, the last layer used linear regression. The architecture of the suggested approach is shown in Fig. 1.

#### 3.1. Data Denoising by Proposed FilterNet Approach

To filter noise, obliterate extraneous data, and maintain the dominant frequency, trained convolutional layers were used in this study. The produced FilterNet was built by a convolution layer with a bottleneck structure integrated with skip connection, dropout, and shuffling approaches for denoising observed vibration signals by employing neural network.

As shown in Fig. 2, the proposed Filter Net had an input layer, convolutional layers, and an output layer as part of its design. For input signals that will be denoised, there were as many neurons in the input and output layers as there were sample points. There were three compression layers, one bottleneck layer, three reconstruction layers, and a final resizing layer among the convolutional layers. Convolution of the input and nonlinear activation of the output using a leaky rectifier were the two operations involved in the compression layers and bottleneck layer, respectively. Convolution of the input features, nonlinear activation of the output using a leaky

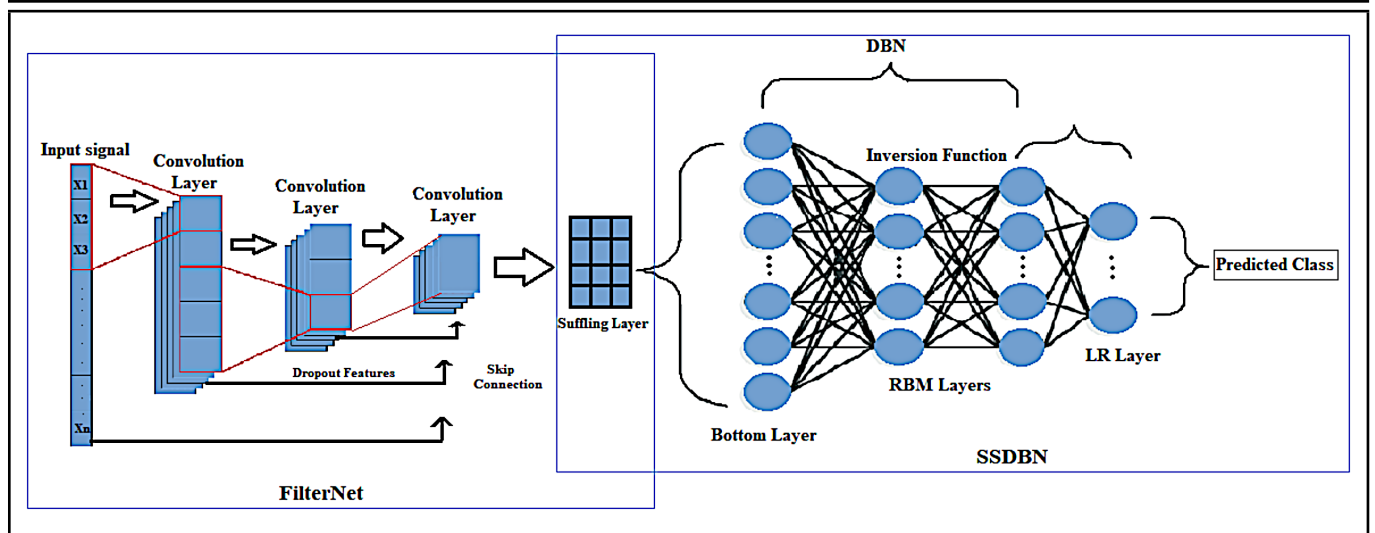


Figure 1. Architecture of the proposed approach.

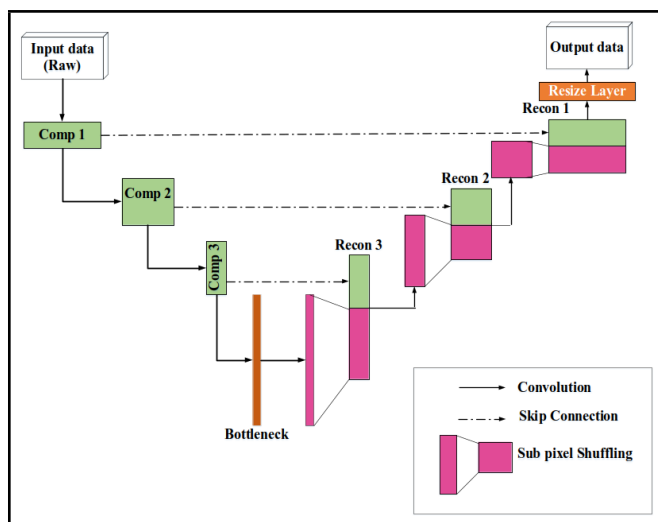


Figure 2. Architecture of FilterNet with a bottleneck structure.

rectifier, resizing of the active output by sup-pixel shuffling, and resizing of the output were the four operations that make up the reconstruction layers. The activated output was finally concatenated with the features of the compression layer in the reversed position (skip connection). The convolution and resizing processes are also included in the final layer.

By continuously deleting the higher-level representation of input signals and utilising convolution kernels with a stride of two, the compression and bottleneck layers lower the dimension of feature maps. To accommodate the higher-level features, the number of feature maps was gradually being increased. The output feature maps from the Bottleneck layer have the smallest dimensionality yet match the highest level of input data features.

One major problem with deep learning-based methods is that, as network depths increase, accuracy may eventually start to saturate and even degrade. Henceforth, a dropout layer ( $p=0.5$ ) was proposed in this research to address the overfitting concerns. Dropout is the term used when neurons separate from the nearby input and output layers and eventually stop functioning. During training with a certain batch of samples,

neurons in networks were randomly killed to distinguish the co-adapted groups of neurons. The network’s generalisation ability was improved because of the more robust training of the remaining neurons. Following that, FilterNet reconstructs output denoised signals by using reconstruction layers only to take account representative information from input signals. The dimension steadily increases and the number of feature maps decreases as a result of the reconstruction layers.

To implement the skip connection, the lengths of feature maps in bottom layers to higher layers should be consistent. The output feature maps from the matched compression layer were twice as large even though they were just a fraction of the length of those from the reconstruction layer. The sub-pixel shuffling operation was involved to resize the output feature maps from the reconstruction layers. Two feature maps from each of the two sets of feature maps were then combined by interpolation to create a single map. It is an instance of a sub-pixel convolution layer in one dimension. Compared to de-convolution, this was a more efficient procedure for shuffling.

Moreover, Skip connections were implemented by concatenating output features from the compression and reconstruction layers in mirrored locations. The paired original and noisy signals were quite similar especially when only a low level of noise exists in the noisy signal. Due to the symmetric architecture of FilterNet, the layers in the mirrored position were sharing many features such as the waveform and structural frequencies information. In order to replace the additional information lost during convolution, the characteristics retrieved from lower layers are effectively shuttled to top layers via the skip links between each pair of layers. This prevented gradient disappearing and made it possible to train deeper networks effectively since it enables gradients to be directly returned to lower layers.

Consequently, the shuffling method upscale feature maps, the suggested FilterNet approach dropout strategy lessened model overfitting, and it also effectively achieved the goal of de-convolution. The model’s training effectiveness was greatly improved by skip connection. Then, the denoised data’s were

fed into the proposed SSDBN model which is described in the following section.

### 3.2. Structural Damage Identification Based on SSDBN Model

A deep neural network (DBN) is a class of multiple-hidden-layer probabilistic generative graphical models. The hidden layer of each sub-network is separated as the visible layer for the succeeding, making the DBN resemble a stack of RBM networks. A DBN has  $l$  layers that RBMs trained. In order to control its probability distribution, an energy function  $E$  with the parameter set as  $\lambda = \{W, b, c\}$ .

$$E(vis, hid; \lambda) = - \sum_{i=1}^m c_i vis_i - \sum_{j=1}^n b_j hid_j - \sum_{i=1}^m \sum_{j=1}^n vis_i hid_j w_{ij}; \quad (1)$$

where  $vis_i$  denotes the binary state of the visible unit  $i$ ;  $hid_j$  represents the binary state of the hidden unit  $j$ ;  $c_i$  represents the bias weight of  $vis_i$ ;  $b_j$  denotes the corresponding bias weight of  $hid_j$ ;  $w_{ij}$  is the collection weight of the hidden layer  $hid_j$  and the visionary layer  $vis_i$ ;  $m$  and  $n$  denote the total number of the visible and hidden units, respectively; and  $\lambda$  represents the model parameter of the RBM.

The joint probability of the state  $prob(vis, hid)$  can be determined using Eq. (1) energy function, stated the following.

$$prob(vis, hid; \lambda) = \frac{e^{-E(vis, hid; \lambda)}}{z(\lambda)}; \quad (2)$$

$$z(\lambda) = \sum_{(v,h)} e^{-E(vis, hid; \lambda)}; \quad (3)$$

Here,  $z$  is a partition function specified in Eq. (3) that enables Eq. (3) sum of the probability distribution to equal 1. Training the RBM entails changing the model parameter based on the training examples. It can be shown from Eq. (3) that altering the model parameter  $\lambda$  would result in a drop or rise in the likelihood of the data  $v$ .

Contrastive divergence (CD) is a new approach that has been developed to obtain the joint probability. A training method to approximate the graphical slope showing the correlation between a network’s weights and error is contrastive divergence. This technique is crucial to demonstrate RBM’s how to activate their “hidden” nodes appropriately, then to adjust their trigger parameters based upon input feedback and continually repeat this dimension reduction process. A few Gibbs sampling steps are all that are necessary to estimate the gradient information when employing the CD approach. As a result, the complicated derivation procedure has been shown in equation using the CD approach.

$$\begin{cases} w_{ij}^t &= w_{ij}^{t-1} + \eta (\langle vis_i hid_j \rangle_{data} - \langle vis_i hid_j \rangle_{recon}) \\ c_i^t &= c_i^{t-1} + \eta (\langle vis_i \rangle_{data} - \langle vis_i \rangle_{recon}) \\ b_j^t &= b_j^{t-1} + \eta (\langle hid_j \rangle_{data} - \langle hid_j \rangle_{recon}) \end{cases}; \quad (4)$$

where  $\eta$  represents the step size;  $\langle \rangle_{data}$  represents that the probability distribution of  $prob(vis, hid; \lambda)$  and  $\langle \rangle_{recon}$  refers to the probability in relation to the model distribution. As a result, the RBM has the flexibility to select the hidden layers.

The whole training process contained two stages. The first stage, namely, “pretraining,” was based on the greedy algorithm to obtain the initial value. The second stage was called “fine tuning,” which generally utilized the supervised algorithm to obtain the final network parameters.

For the following layers, the greedy learning algorithm was employed to train the network, with the corresponding input defined as the activation of the hidden layer in the previous subnetwork. A composite model was developed by using the stacked RBMs. The top two layers were defined as the RBM, and the lower one a direct belief net. This hybrid model was named after DBN, with the probability function calculated as:

$$prob(x_0, hid_1, hid_2, \dots, hid_L) = prob(hid_{L-1}, hid_L) \cdot prob(vis | hid_1) \prod_{L=2}^{L-1} prob(hid_{L-1} \vee hid_L). \quad (5)$$

The first RBM’s parameters,  $x_0$  and  $h_1$ , were developed using the observed data  $x_0$ , where  $x_0$  denotes the observed data and  $prob(hid_{L-1} \vee hid_L)$  denotes the conditional probability of  $hid_{L-1}$  given  $hid_L$ .  $prob(hid_{L-1} \vee hid_L)$  is the joint probabilistic distribution, which can also be viewed as a RBM’s probability distribution with the visible unit  $hid_{L-1}$  and the hidden unit  $hid_L$ .

There were two parts to the entire training procedure. The greedy algorithm was used in the first stage, known as “pre-training,” to determine the starting value. The final network parameters were often obtained during the second step, which was referred to as “fine tuning,” which used the supervised technique.

An example of an unsupervised method was the greedy algorithm, which trains the first RBM (which is made up of the data  $x$  and  $h_1$ ) using sampling data. The parameters of the first RBM are then used to initialise the parameters of the DBN’s first layer. The DBN’s input for the first RBM is determined using Eq. (4). When  $L$  layers have been added, the recently computed output will be used as the first layer’s input. The Back Propagation network was then used to derive the ultimate systematic parameters in a fine-tuning procedure that was then added. The characteristics from the compression layer’s final concatenation are activated in the output visible layer in the reversed position.

Finally, the linear regression layer was used to identify the structural damage from vibrational data. In this instance, 30% of the data was being used for testing and 70% for training. The equation of the linear regression is as follows:

$$\hat{y} = U_0 + U_1 X_1 + U_2 X_2 + U_3 X_3 + \dots U_m X_m + \epsilon; \quad (6)$$

where  $\hat{y}$  is the dependent variable’s anticipated or forecast value;  $X_1$  through  $X_m$  are  $m$  separate predictor or independent variables;  $U_0$  is the value of  $\hat{y}$  when every independent

**Table 1.** Parameters of the proposed FilterNet.

Layer	Kernel number	Kernel size	Stride	Padding	Input shape	Output shape	Shuffling
Input	—	—	—	—	(1,944)	(1,944)	—
Comp 1	128	64	2	Same	(1,944)	(128,512)	N
Comp 2	256	32	2	Same	(128,512)	(256,256)	N
Comp 3	512	16	2	Same	(256,256)	(512,128)	N
Bottleneck	944	8	2	Same	(512,128)	(944,64)	N
Recon 3	944	16	1	Same	(944,64)	(944,128)	Y
Recon 2	512	32	1	Same	(944,128)	(512,256)	Y
Recon 1	256	64	1	Same	(512,256)	(256,256)	Y
Final	2	8	1	Same	(256,512)	(1,944)	Y
Output	—	—	—	—	(1,944)	(1,944)	—

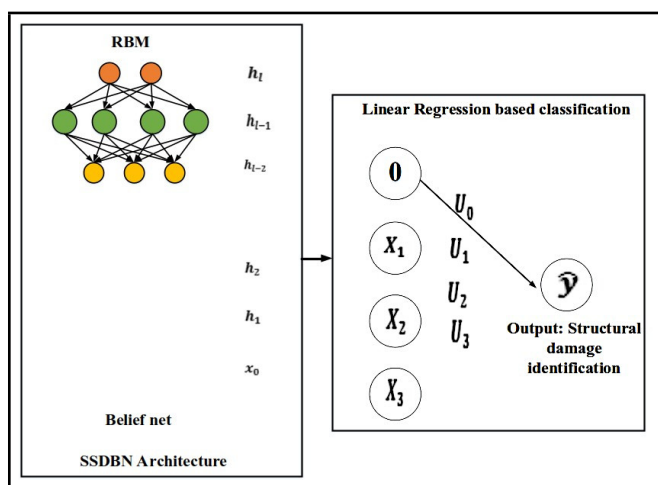


**Figure 3.** Structural Damage Identification based on SSDBN Model.

variable ( $X_1$  through  $X_m$ ) equals zero;  $U_1$  through  $U_m$  are calculated regression coefficients,  $\varepsilon$  — random error. Figure 3 depicts the structural damage identification based on SSDBN Model.

As a result, our research offers a greater performance in terms of accuracy by utilising the suggested SSDBN model. In addition, the findings obtained by utilising our technique are presented in the following part.

### 4. ACQUIRED RESULTS

This section details the performance and comparative findings of the suggested strategy, as well as the implementation outcomes

**Tool:** PYTHON 3

**OS:** Windows 7 (64 bit)

**Processor:** Intel Premium

**RAM:** 8GB RAM

#### 4.1. Dataset Description

The dataset used in this study was compiled using sensor readings taken from the Vibration Database.<sup>20</sup> Here, PCB

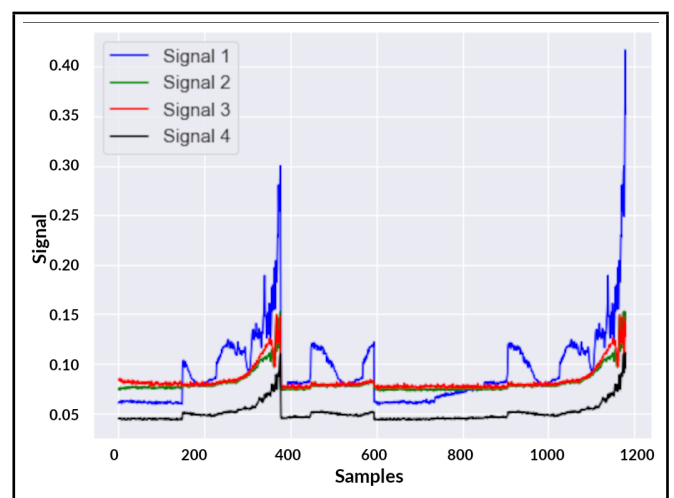


**Figure 4.** Various signals from the vibrational data.

353B33 High Sensitivity Quartz ICP accelerometers were installed on the housing of each bearing. For each bearing two accelerometers were installed in radial directions, orthogonal to each other; in this study, sensor measurements were acquired on four signals that were continuously loaded over a period of days until they failed. Each file in our dataset is a snapshot of a 1-second vibration signal that was recorded at 10-minute intervals. Each file has 20,480 sensor data points since the sensors are read at a 20 kHz sampling rate. Figure 4 illustrates the 4 signals that make up this dataset at various times.

#### 4.2. Performance Measures

The various performance metrics of the suggested deep learning system for tracking structural health are described in this section.

Using our proposed FilterNet with integrated skip connection, dropout, and shuffle techniques for de-noising observed vibration signals, which is shown in Fig. 5, the training loss of the recommended method is 0.012 at epoch 5.

Using our proposed FilterNet with integrated skip connection, dropout, and shuffling algorithms for denoising observed vibration signals, as shown in Fig. 6, the testing loss of the

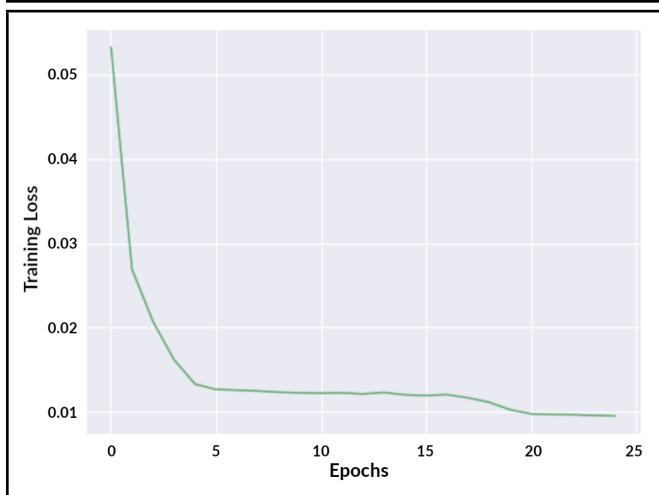


Figure 5. Training loss of the proposed approach.

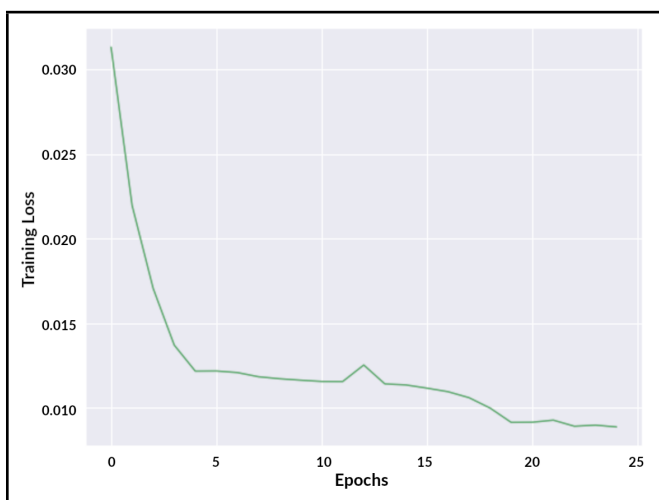


Figure 6. Testing loss of the proposed approach.

recommended strategy is 0.0122 at epoch 5.

Structural damage identification results of the proposed Smooth Sparse Deep Boltzmann Network is depicted in Fig. 7. Figure 7 identifies the structural damage in the signal dataset. A confusion matrix displays the appropriately recognised structural damage on the primary diagonal (top left to bottom right). In the additional cells, known as true negatives or false negatives, the erroneous labels are visible. The suggested hybrid model therefore produces superior outcomes. From that confusion matrix, we obtain the following performance values.

A number of measures, including recall, accuracy, F1 Score, and precision are used to evaluate the efficacy of our proposed method as well as the presentation of the method. The formulae described below are used to compute the performance metrics Accuracy, Precision, Recall, and F1 Score.

$$\text{Accuracy} = \frac{TP + TN}{TP + TN + FP + FN}; \tag{7}$$

$$\text{Precision} = \frac{TP}{TP + FP}; \tag{8}$$

$$\text{Recall} = \frac{TP}{TP + FN}; \tag{9}$$

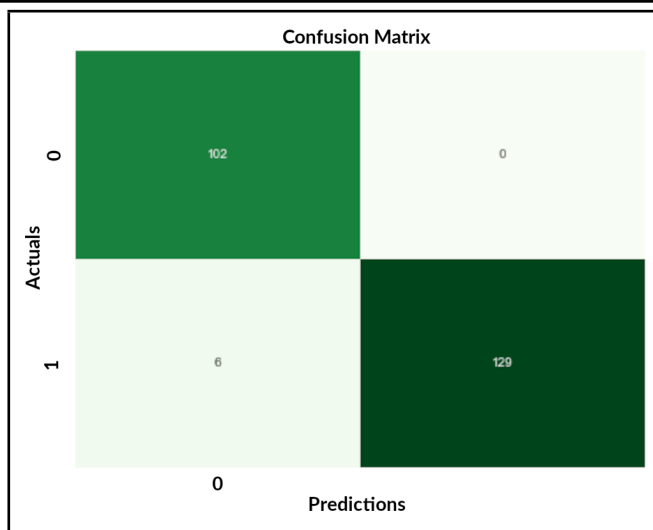


Figure 7. Results of structural damage identification.

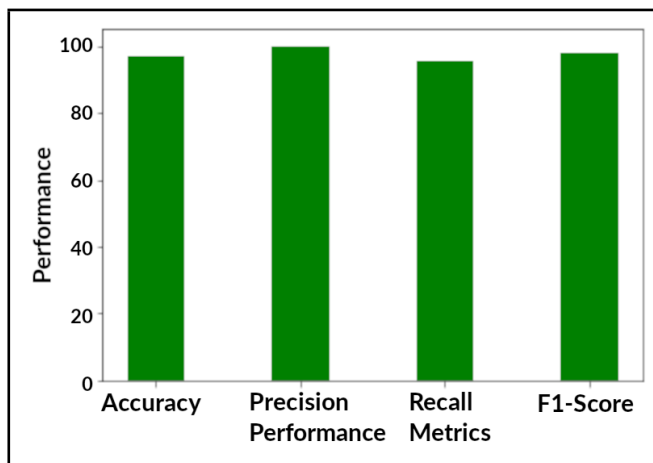


Figure 8. Proposed approach performance results.

$$\text{F1 Score} = \frac{2 * \text{Precision} * \text{Recall}}{\text{Precision} + \text{Recall}}; \tag{10}$$

where  $TP$  is true positive,  $TN$  is true negative,  $FP$  is false positive and  $FN$  is false negative.

The suggested method’s performance evaluation measures are shown in Figure 8. The results were 97% accuracy, 97.73% F1 score, 100% precision, and 95.56% recall. By implementing a unique Smooth Sparse Deep Boltzmann Network, Accuracy, F1 score, precision, and recall are all improved by our proposed approach.

### 4.3. Comparison Results

The suggested strategy is compared to standard methods like K-Nearest Neighbour (KNN), C-Support Vector Classifier

Table 2. Accuracy Comparison.

Methods	Data	Accuracy (%)
KNN	Crack	94.6
SVC	Crack	89.3
SVMH	Crack	85.5
KNN	Corrosion	82.8
SVMH	Corrosion	84.0
Proposed	Crack	97

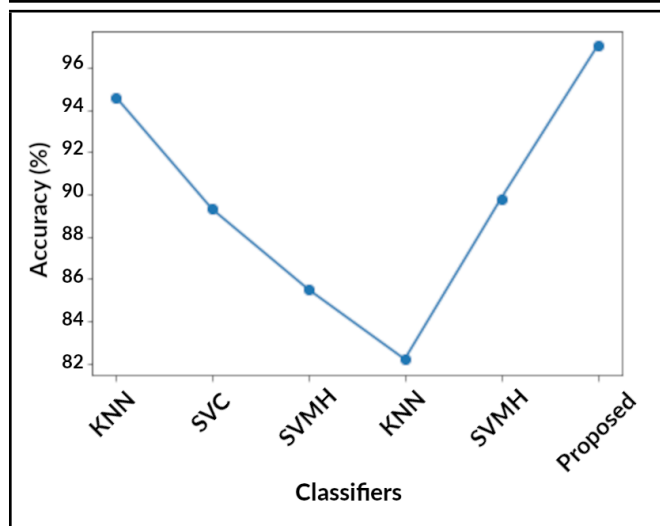


Figure 9. Comparison methods on structural damage detection accuracy.

Table 3. F1-Score Comparison.

Methods	Data	Accuracy (%)
KNN	Crack	92.6
SVC	Crack	84.3
SVMH	Crack	83.5
KNN	Corrosion	82.2
SVMH	Corrosion	88.8
Proposed	Crack	97.73

(SVC), and Linear Support Vector Classifier (SVMH) in this part that deals with the comparison of the current techniques.<sup>19</sup>

Figure 9 displays the total accuracy comparison. Using Smooth Sparse Deep Boltzmann Network enhances the suggested method’s accuracy. Our proposed method outperforms the baseline K-Nearest Neighbour (KNN), C-Support Vector Classifier (SVC), Linear Support Vector Classifier (SVMH), K-Nearest Neighbour (KNN), and Linear Support Vector Classifier (SVMH) for crack, corrosion, and corrosion, respectively, with accuracy rates of 94.6%, 89.3%, 85.5%, and 82%. Our unique, revolutionary approach has a 97% accuracy rate, which is higher than conventional approaches.

Figure 10 displays a comparison of all F1 scores. By in-

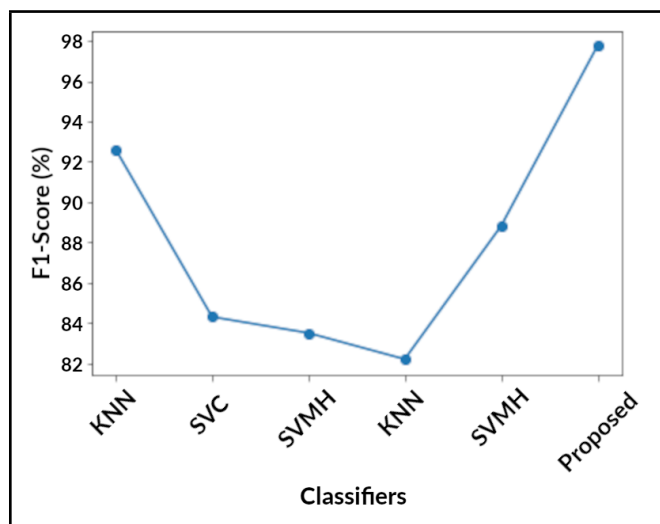


Figure 10. Comparison methods on structural damage detection F1-Score.

cluding a linear regression layer into a smooth sparse deep Boltzmann network, the F1-score of the suggested method is increased. Comparing our proposed strategy to the baseline, we find that higher F1-scores for crack data, corrosion data, and crack data using K-Nearest Neighbour (KNN), C-Support Vector Classifier (SVC), Linear Support Vector Classifier (SVMH), and K-Nearest Neighbour (KNN), respectively, with 92.6%, 84.3%, 83.5%, 82.2%, and 88.8%. As a conclusion, our novel, original strategy performed better than baseline procedures with an F1-score of 97.73%.

### 5. CONCLUSION

This study develops a novel deep learning framework to overcome the problems such as strong noise in the vibrational data, accuracy saturation, and a need of large amount of data. To filter the noise, obliterate extraneous data, and maintain the dominant frequency this research proposes a FilterNet which is integrated with skip connection, dropout and shuffling layer. As a result, the FilterNet provides reconstructed signals by effectively denoising of input signals. Moreover, to identify the structural damage from the denoised data, this research proposes a Smooth Sparse Deep Boltzmann Network. The proposed network identifies the structural defects by the enormous accuracy. Moreover, our research compares the proposed approach to the baseline approach since the proposed approach provides the best representation and enhances the system’s performance. The suggested findings of this study are significant, with an accuracy of 97% by using the signal dataset which is extremely effective in detecting structural damage.

### REFERENCES

- 1 Tiachacht, S., Khatir, S., Thanh, C. L., Rao, R. V., Mirjalili, S., and Abdel Wahab, M. Inverse problem for dynamic structural health monitoring based on slime mould algorithm. *Engineering with Computers*, 1–24, (2021). <https://doi.org/10.1007/s00366-021-01378-8>
- 2 Sivasuriyan, A., Vijayan, D. S., Górski, W., Wodzyński, Ł., Vaverková, M. D., and Koda, E. Practical implementation of structural health monitoring in multi-story buildings. *Buildings*, 11(6), 263, (2021). <https://doi.org/10.3390/buildings11060263>
- 3 Zhang, Y. M., Wang, H., Wan, H. P., Mao, J. X., and Xu, Y. C. Anomaly detection of structural health monitoring data using the maximum likelihood estimation-based Bayesian dynamic linear model. *Structural Health Monitoring*, 20(6), 2936–2952, (2021). <https://doi.org/10.1177/1475921720977020>
- 4 Malekloo, A., Ozer, E., AlHamaydeh, M., and Girolami, M. Machine learning and structural health monitoring overview with emerging technology

- and high-dimensional data source highlights. *Structural Health Monitoring*, **21**(4), 1906–1955, (2022). <https://doi.org/10.1177/14759217211036880>
- <sup>5</sup> Chen, X., Semenov, S., McGugan, M., Madsen, S. H., Yeniceli, S. C., Berring, P., and Branner, K. Fatigue testing of a 14.3 m composite blade embedded with artificial defects—damage growth and structural health monitoring. *Composites Part A: Applied Science and Manufacturing*, **140**, 106189, (2021). <https://doi.org/10.1016/j.compositesa.2020.106189>
  - <sup>6</sup> Lei, X., Sun, L., and Xia, Y. Lost data reconstruction for structural health monitoring using deep convolutional generative adversarial networks. *Structural Health Monitoring*, **20**(4), 2069–2087, (2021). <https://doi.org/10.1177/1475921720959226>
  - <sup>7</sup> Mao, J., Wang, H., and Spencer Jr, B. F. Toward data anomaly detection for automated structural health monitoring: Exploiting generative adversarial nets and autoencoders. *Structural Health Monitoring*, **20**(4), 1609–1626, (2021). <https://doi.org/10.1177/1475921720924601>
  - <sup>8</sup> Mariani, S., Rendu, Q., Urbani, M., and Sbarufatti, C. Causal dilated convolutional neural networks for automatic inspection of ultrasonic signals in non-destructive evaluation and structural health monitoring. *Mechanical Systems and Signal Processing*, **157**, 107748, (2021). <https://doi.org/10.1016/j.ymssp.2021.107748>
  - <sup>9</sup> Fan, G., Li, J., and Hao, H. Dynamic response reconstruction for structural health monitoring using densely connected convolutional networks. *Structural Health Monitoring*, **20**(4), 1373–1391, (2021). <https://doi.org/10.1177/147592172091>
  - <sup>10</sup> Wang, R., Chenchao, An, S., Li, J., Li, L., Hao, H., and Liu, W. Deep residual network framework for structural health monitoring. *Structural Health Monitoring*, **20**(4), 1443–1461, (2021). <https://doi.org/10.1177/1475921720918>
  - <sup>11</sup> Svendsen, B. T., Frøseth, G. T., Øiseth, O., and Rønnquist, A. A data-based structural health monitoring approach for damage detection in steel bridges using experimental data. *Journal of Civil Structural Health Monitoring*, **12**(4), 1–15, (2022). <https://doi.org/10.1007/s13349-021-00530-8>
  - <sup>12</sup> Hughes, A. J., Bull, L. A., Gardner, P., Barthorpe, R. J., Dervilis, N., and Worden, K. On risk-based active learning for structural health monitoring. *Mechanical Systems and Signal Processing*, **167**, 108569, (2022). <https://doi.org/https://doi.org/10.1016/j.ymssp.2021.108569>
  - <sup>13</sup> Hubbard, P. G., Xu, J., Zhang, S., Dejong, M., Luo, L., Soga, K., and Minto, C. Dynamic structural health monitoring of a model wind turbine tower using distributed acoustic sensing (DAS). *Journal of Civil Structural Health Monitoring*, **11**(3), 1–17, (2021). <https://doi.org/10.1007/s13349-021-00483-y>
  - <sup>14</sup> Sivasuriyan, A., Vijayan, D. S., Górski, W., Wodzyński, Ł., Vaverková, M. D., and Koda, E. Practical implementation of structural health monitoring in multi-story buildings. *Buildings*, **11**(6), 263, (2021). <https://doi.org/10.3390/buildings11060263>
  - <sup>15</sup> Maes, K., Van Meerbeeck, L., Reynders, E. P. B., and Lombaert, G. Validation of vibration-based structural health monitoring on retrofitted railway bridge KW51. *Mechanical Systems and Signal Processing*, **165**, 108380, (2022). <https://doi.org/10.1016/j.ymssp.2021.108380>
  - <sup>16</sup> Liu, G., Li, P., Wang, P., Liu, J., Xiao, J., Chen, R., and Wei, X. Study on structural health monitoring of vertical vibration of ballasted track in high-speed railway. *Journal of Civil Structural Health Monitoring*, **11**, 451–463, (2021). <https://doi.org/https://doi.org/10.1007/s13349-020-00460-x>
  - <sup>17</sup> Jahan, S., Mojtahedi, A., Mohammadyzadeh, S., and Hokmabady, H. A fuzzy Krill Herd approach for structural health monitoring of bridges using operational modal analysis. *Iranian Journal of Science and Technology, Transactions of Civil Engineering*, **45**, 1139–1157, (2021). <https://doi.org/10.1007/s40996-020-00475-w>
  - <sup>18</sup> Bedon, C., Bergamo, E., Izzi, M., and Noè, S. Prototyping and validation of MEMS accelerometers for structural health monitoring—The case study of the Pietratagliata cable-stayed bridge. *Journal of Sensor and Actuator Networks*, **7**(3), 30, (2018). <https://doi.org/10.3390/jsan7030030>
  - <sup>19</sup> Wu, R. T., Singla, A., Jahanshahi, M. R., Bertino, E., Ko, B. J., and Verma, D. Pruning deep convolutional neural networks for efficient edge computing in condition assessment of infrastructures. *Computer-Aided Civil and Infrastructure Engineering*, **34**(9), 774–789, (2019). <https://doi.org/10.1111/mice.12449>
  - <sup>20</sup> Cavalaglio Camargo Molano, J., Strozzi, M., Rubini, R., and Coconcelli, M. Analysis of nasa bearing dataset of the university of cincinnati by means of hjorth’s parameters. In Proceedings of the International Conference on Structural Engineering Dynamics ICEDyn 2019, (2019).